AJNR

Proton MR spectroscopic characteristics of pediatric pilocytic astrocytomas.

J H Hwang, G F Egnaczyk, E Ballard, R S Dunn, S K Holland and W S Ball, Jr

AJNR Am J Neuroradiol 1998, 19 (3) 535-540
http://www.ajnr.org/content/19/3/535

AJNR Am J Neuroradiol 19:535–540, March 1998

Proton MR Spectroscopic Characteristics of Pediatric Pilocytic Astrocytomas

Jong-Hee Hwang, Greg F. Egnaczyk, Edgar Ballard, R. Scott Dunn, Scott K. Holland, and William S. Ball, Jr

PURPOSE: **We report the common characteristics of juvenile pilocytic astrocytomas revealed by proton MR spectroscopy.**

METHODS: **Eight children with pilocytic astrocytomas were studied with proton MR spectroscopy. The selected sampling volume was approximately 4 cm^3, obtained from solid tumor. To localize the sampling volume, we used point-resolved spectroscopy (PRESS) and stimulated-echo acquisition mode (STEAM) techniques to acquire long- and short-TE spectra, respectively. Spectra from PRESS and STEAM sequences were processed using Lorentzian-to-Gaussian transformation and exponential apodization, respectively. For PRESS (2000/270) spectra, peaks of creatine, choline, *N*-acetylaspartate (NAA), and lactate resonances were integrated; for STEAM (2000/20) spectra, we measured the amplitude of the peaks at 3.2, 2.0, 1.3 and 0.9 ppm.**

RESULTS: **An elevated lactate doublet was observed in the PRESS spectra. The choline/NAA ratio was 3.40. The amplitude ratios of the lipid pattern (0.9, 1.3 and 2.0 ppm) to choline were all below one.**

CONCLUSION: **Despite the benign histology of the tumor, which generally lacks necrosis, a lactate signal was detected in all eight patients studied. A dominant lipid pattern was not observed.**

Magnetic resonance (MR) imaging has become an essential tool in the diagnosis and evaluation of primary brain tumors (1). However, MR imaging has shown only a limited capability in the assessment of a tumor's grade or histology. In vivo MR spectroscopy provides complementary information on tumor metabolism, which may assist in tumor grading and enable better understanding of biochemical pathways within the tumor.

Recently, the use of short-echo-time (TE) proton MR spectroscopy has allowed the observation of macromolecules and lipids (2–5), in addition to the small molecular metabolites, such as *N*-acetylaspartate (NAA), choline (Cho), and lactate. Since Kuesel et al (6) reported a positive correlation between the lipid content and necrosis in high-grade astrocytomas, lipids have been recognized as potential indicators of malignancy. Because the T2 signals of lipids and macromolecules are very short, short-TE proton MR spectroscopy is required for their detection (2–4). In addition, lactate is often identified within tumors, which may indicate necrosis and ischemia, or it may be the product of primary metabolic pathways involving lactate, such as anaerobic glycolysis.

Juvenile pilocytic astrocytoma is one of the most common brain tumors found in children. In this study, we used two single-voxel proton MR spectroscopic methods to investigate pediatric pilocytic astrocytomas: a long-TE point-resolved spectroscopic (PRESS) sequence for small-molecule metabolites, and a short-TE stimulated-echo acquisition mode (STEAM) sequence for lipids and macromolecules as well as for the small-molecule metabolites. Our objective was to identify the common proton MR spectroscopic characteristics of juvenile pilocytic astrocytomas in a group of children.

Methods

Eight patients ranging in age from 1 to 12 years (mean, 6.8 ± 2.6 years) were studied. All patients had MR images showing brain tumors in the region of the cerebellum, and subsequent pathologic analysis of surgical tissue provided histologic confirmation of the diagnosis of juvenile pilocytic astrocytoma in each case. No exceptional findings or atypical histologic features in the pilocytic tumor group were observed by routine histopathologic evaluation of the tumors. The data were collected during the years 1992 to 1996. At the time of the study, none of the patients had received radiotherapy or chemotherapy.

Proton MR spectroscopy was performed on a 1.5-T clinical whole-body system before administration of contrast medium.

Received May 22, 1997; accepted after revision October 20.

Supported in part by a grant from GE Medical Systems.

From the Imaging Research Center, Departments of Radiology (J-H.H., R.S.D., S.K.H., W.S.B.), Pediatrics (J-H.H., E.B., S.K.H., W.S.B.), and Pathology (E.B.), Children's Hospital Medical Center, MD/PhD Program (G.F.E.), University of Cincinnati (Ohio).

Address reprint requests to Jong-Hee Hwang, PhD, Imaging Research Center, Department of Radiology, Children's Hospital Medical Center, 3333 Burnet Ave, Cincinnati, OH 45229.

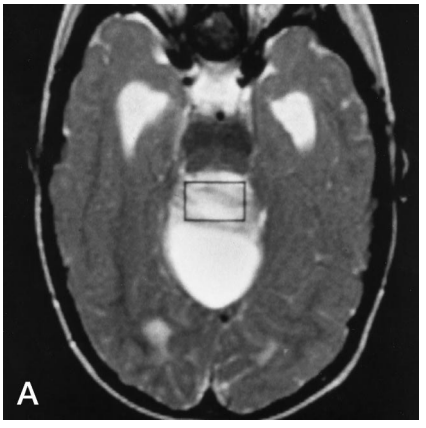

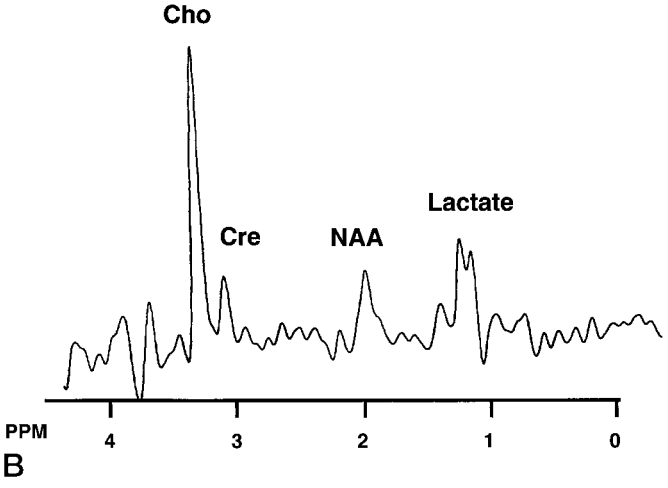

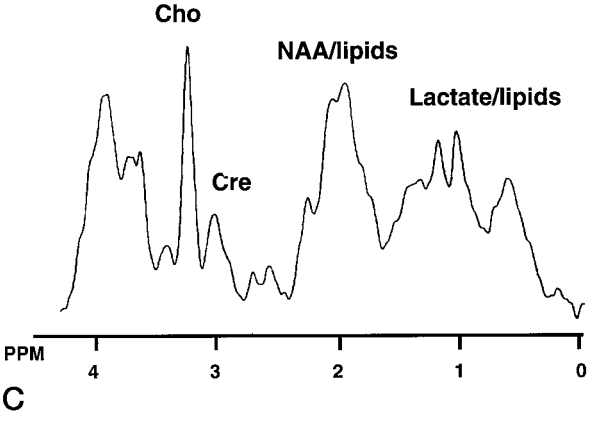

FIG 1. Long- and short-TE spectra of a pilocytic tumor in a 16-month-old boy.

A, Axial T2-weighted image (2800/100) shows the cerebellar pilocytic tumor and selected volume (3.6 cm^3) for proton MR spectroscopy.

B, Proton spectrum from PRESS sequence (2000/270) in pediatric pilocytic astrocytoma. Decreased NAA (2.0 ppm) and Cr (3.0 ppm) were observed, and lactate (1.33 ppm) and Cho (3.2 ppm) are prominent. The lactate doublet (coupling constant, 7.5 Hz) is clearly visible.

C, Proton spectrum from STEAM sequence (2000/20; TM = 13.7) shows broadened peaks from short T2 components and overlapped peaks with lipids and macromolecules; however, Cho peak (3.2 ppm) is still prominent.

All MR imaging and spectroscopic acquisitions were obtained with a quadrature head coil. All eight patients were sedated for the procedure with pentobarbital (3 to 6 mg/kg) and, once sedated, were monitored by EKG and pulse oximetry during the examination. Informed consent was obtained from the parents in all cases. MR images were used to localize the voxel for spectral acquisition in tumor tissue. The voxel size for spectroscopy was approximately $1.5 \times 1.5 \times 1.5$ cm^3 to ensure that the region of interest was totally within solid tumor. Great care was taken to avoid any contamination of the voxel from normal tissue or tumor cysts. Three of the eight tumors were entirely solid; the remaining five tumors consisted of a solid nodule associated with a single macrocyst or a multiseptated cyst. The dimensions of the nodules in two of the tumors were over $5 \times 5 \times 5$ cm^3; in four cases, the nodules were approximately $3 \times 3 \times 3$ cm^3, in one case it was $3 \times 3 \times 1.5$ cm^3, and in one case the nodule was $1.5 \times 1.5 \times 1.5$ cm^3. Thus, in seven of eight cases, the selected voxel size for spectroscopy was at least two to three times smaller than the solid portion of the tumors. In only one case did the voxel approach the same size as the solid portion of the tumor.

Before acquiring spectra, we optimized transmitter gains of the 90° and 180° pulses and also used linear shim coils to optimize shimming. Water signals were suppressed by using a chemical-shift selective (CHESS) pulse sequence before applying the localization pulses (7). The third CHESS pulse was adjusted to suppress water maximally. A PRESS sequence (8) for a long-TE (270 milliseconds) and a STEAM sequence (9, 10) for a short-TE (20 milliseconds; TM, 13.7 milliseconds) were used to obtain the spectra. A spectral width of 2000 Hz or 2500 Hz was used, and the data size in the time domain was 2K. One hundred ninety-two and 128 scans were obtained for the PRESS and STEAM sequences, respectively. The TR was 2 seconds for both methods.

Data processing and analysis were performed on a Sun workstation using SA/GE software (GE Medical Systems, Milwaukee, Wis). Processing of data from the PRESS sequences was done by the Lorentzian-to-Gaussian transformation. Since the characteristics of the short-TE spectrum are different from those of the long-TE spectrum, the free induction decay from the short-TE STEAM sequence was processed using only exponential apodization with line broadening of 3 Hz.

Data analysis entailed calculation of the metabolites' peak areas for the data from the PRESS sequence. A modified version of the SA/GE program was used to perform a Marquardt fit and to integrate selected peaks: lactate (1.3 ppm), NAA (2.0 ppm), creatine (Cr) (3.0 ppm), and Cho (3.2 ppm). Each peak was fitted and integrated over a range of ±0.1 ppm for the spectra. The peak area measurements were used to calculate Cho/NAA, lactate/Cr, NAA/Cr, Cho/Cr, and lactate/NAA ratios. Peak amplitudes alone were measured in the spectra acquired with the STEAM sequence. The amplitudes at 3.2 ppm (Cho) and at three major lipid peaks (2.0 ppm, 1.3 ppm, and 0.9 ppm) were measured. Since the amplitude for the 3.2 (Cho) peak was reasonably free from lipid signals, this was chosen as a reference for comparison with other lipid pattern peaks. The areas of the peaks were not measured because of broad overlapping resonances of the macromolecules and lipids in the short-TE spectrum.

Means and standard deviations based on the entire population were calculated using Microsoft Excel programs.

Results

Results from Long-TE PRESS Spectroscopy

Figures 1B and 2B show the long-TE PRESS spectrum (270 milliseconds) and the corresponding image

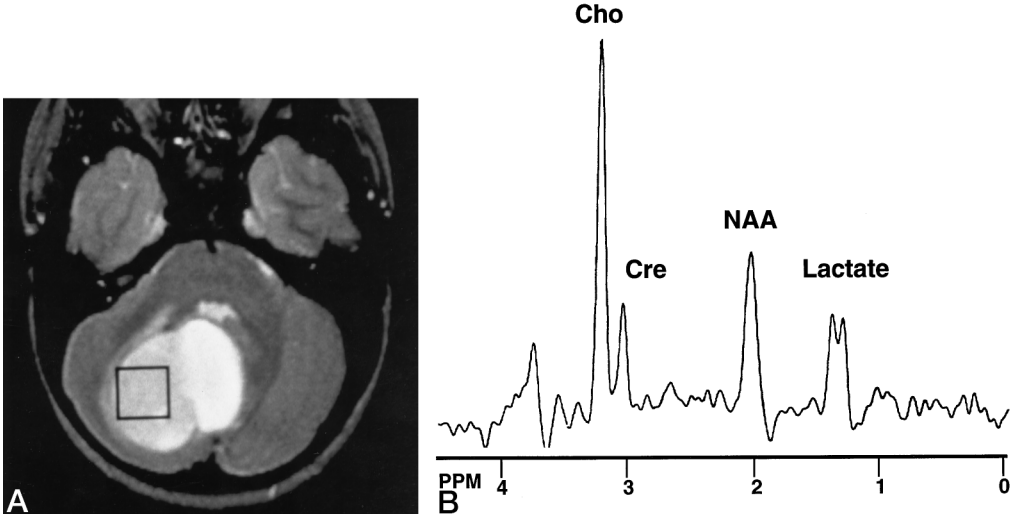

FIG 2. Long-TE spectrum of a cerebellar pilocytic tumor in a 10-year-old boy.
A, Axial T2-weighted image (2800/100) shows selected volume (4.9 cm^3) for spectroscopy.
B, Proton spectrum from PRESS sequence (TE = 270) in pediatric pilocytic astrocytoma shows diminished Cr (3.0 ppm) and NAA (2.0 ppm) and elevated lactate, with a coupling constant 7.5 Hz (1.33 ppm).

for localization within the solid portion of the pilocytic astrocytomas, respectively. Typically, these spectra revealed a high Cho resonance and a clearly delineated lactate doublet at 1.33 ppm, whereas the Cr and NAA resonances were diminished. The lactate doublet resonances were observed in all patients. The Cho/NAA ratio is frequently reported in proton MR spectroscopic studies, since it reliably differentiates healthy from diseased brain tissue (11, 12). The average ratio (n = 8) for Cho/NAA of 3.40 is very high compared with the normal values reported previously in the cerebellum of 0.75 and 0.84 (11, 12), which could reflect either an elevation of Cho or a decrease of NAA in the tumor. Elevated lactate was found relative to Cr and NAA; lactate/Cr and lactate/NAA were 2.69 and 1.74, respectively. In six cases, the ratios of NAA/Cr and Cho/Cr were 1.55 and 3.46, respectively. In two cases, with minimal Cr peaks, those ratios resulted in an infinitely high value and were not included in the calculation of the average Cho/Cr and NAA/Cr ratios, as indicated in the Table. The value of NAA/Cr (1.55) was very close to the values of 1.49 and 1.55 reported for pilocytic tumor and normal tissue, respectively (11). Comparisons between our data and those from other studies are found in the Table.

Results from Short-TE STEAM Spectroscopy

The spectrum from the STEAM sequence (TE = 20, TM = 13.7) is shown in Figure 1C. Since spectral peaks obtained with a short TE are not as well resolved as those obtained with a long TE, owing to the overlapping peaks from macromolecules and lipids, only the relative amplitude ratios were measured. Measurements were made at 0.9 ppm, 1.3 ppm, and 2.0 ppm relative to 3.2 ppm (Cho) in order to examine the dominance of lipids in the short-TE spectrum (3). In a short-TE proton spectrum, peaks at about 1.3 ppm are composed mainly of methylene protons of neutral lipids, and lactate. Peaks at about 2.0 ppm represent lipid and cytosolic protein macromolecules,

Comparison of current and previous results from long-TE (270 ms) single-voxel spectroscopic studies and extracts of pilocytic tumors

Author	Location of Tumors	Description	Metabolic Ratios				Voxel Size, mm	Imaging Sequence
			Cho/NAA	Cho/Cr	Lactate/Cr	NAA/Cr		
Current work	All in the cerebellum	Pilocytic astrocytoma	3.40 ± 2.14	3.46 ± 1.49	2.69 ± 1.91	1.55 ± 0.61	~15 × 15 × 15	PRESS
Sutton et al (11)	Mostly in the cerebellum	Pilocytic astrocytoma	1.80 ± 0.71	2.84 ± 0.20	2.04 ± 1.5	1.55 ± 0.92	~25 × 25 × 25	STEAM
Sutton et al (11)	···	Normal cerebellum	0.75 ± 0.28	1.08 ± 0.35	0.02 ± 0.04	1.49 ± 0.27	~25 × 25 × 25	PRESS STEAM
Sutton et al (12)*	Mostly in the cerebellum	Pilocytic astrocytoma	3.35 ± 0.59	···	···	···	Extract	PRESS Pulse-acquired
Sutton et al (12)*	···	Normal vermis	0.53 ± 0.10	···	···	···	Extract	Pulse-acquired
Lazareff et al (13)	Mostly in the optic chiasm	Pilocytic astrocytoma	2.14	···	···	···	···	PRESS-SI

* The ratios were based on concentrations.
Note.—PRESS indicates point-resolved spectroscopy; STEAM, stimulated-echo acquisition mode; SI, spectroscopic imaging.

whereas peaks at about 0.9 ppm represent methyl protons in lipids and macromolecules (3, 4). The relative ratios of signal intensities at 0.9 ppm, 1.3 ppm, and 2.0 ppm to 3.2 ppm (Cho signals) were measured. All three ratios were less than 1.0; that is, 0.76, 0.95, 0.70, respectively. Since the methylene peak at 1.3 ppm has the strongest signal for lipids, the ratio of $I_{1.3}/I_{3.2}$ (intensity at 1.3 ppm/the intensity at 3.2 ppm) is an important measure of lipids, and was found to be 0.95. Since the intensity at 1.3 ppm in a short-TE proton spectrum also contains a contribution from the elevated lactate doublet, true lipid contribution at 1.3 ppm is even less than the values estimated from the 1.3 ppm/3.2 ppm amplitude ratio in this tumor.

Discussion

Comparisons with Previous Studies of Pediatric Pilocytic Tumors

A comparison of our data with results of other studies (11–13) in which long-TE proton MR spectroscopy was used on both conventional clinical and high-resolution MR systems is shown in the Table.

Cho/NAA and Cho/Cr ratios were found to be 3.40 and 3.46, respectively. The in vivo study of pilocytic astrocytomas using proton MR spectroscopy by Sutton et al (11) showed a Cho/NAA ratio of 1.80, which is smaller than the ratio found in our study and in the study in which tumor extracts were used (12). We also found a higher Cho/Cr ratio than that reported by Sutton et al (11). The value for the Cho/Cr ratio found by Sutton and colleagues was 2.84. Actually, the Cho/Cr ratio of 3.46 can only be considered as a lower limit, because, in two of the tumors, the Cr peak was not measurable, resulting in our Cho/Cr ratio of between 3.46 and infinity. Thus, a consistently higher Cho content was found in our results than in those obtained by Sutton et al (11). The discrepancy may be attributed to several factors. One may be that the larger voxel size used by Sutton et al (about $2.5 \times 2.5 \times 2.5$ cm^3) was 4.6 times greater than the voxel size used in our study. Thus, inclusion of a component of normal tissue may have contributed to their lower ratio. The different pulse sequences used may also have played a role: Sutton et al used both STEAM and PRESS sequences for long-TE (270-millisecond) acquisitions, while we used only PRESS sequences. The use of two different sequences in one study may lead to a problem, because STEAM has a TM period that is influenced by T1 whereas PRESS does not. A difference in TRs was also found between our study and theirs. The NAA/Cr ratio is consistent in both tumors and normal tissues in all studies (11, 12). It has been assumed that residual NAA and Cr might be from surrounding normal tissue; however, a contribution of both NAA and Cr by the tumor itself is supported by the study of tumor extracts (12). As pilocytic tumor is not considered an infiltrative tumor, it is difficult to explain the presence of NAA and Cr by contamination of normal tissue adjacent to the mass or by infiltration of normal tissue by neoplasm. However, an NAA/Cr ratio that we resolved in vivo was very close to the value found in tumor extracts; thus, NAA may exist within the pilocytic tumors as suggested previously by Sutton et al (12). The ratio of lactate/NAA shows the same trend as the ratio of Cho/NAA. Levels of lactate in our patients were considerably higher than those in the in vivo study by Sutton et al (11). Their in vivo work can be directly compared with the data from our PRESS sequence, since both were from a single voxel at the same TE (270 milliseconds). It is presumed that their large voxel selection may have resulted in a larger contribution of normal tissue, resulting in lower Cho/NAA and lactate/NAA ratios (11). Whether the Cho peak itself is actually elevated in pilocytic astrocytomas has also recently come into question. According to Lazareff et al (13), in a spectroscopic imaging study of pilocytic tumors, the Cho signal in the tumor itself may not be elevated relative to the Cho signal from contralateral normal tissue.

In Vivo Lipid Signals and Malignancy of Tumors

Although a minimal elevation of lipids may be present in pilocytic astrocytomas, it is clear that the contribution of the lipid is not high as compared with glioblastoma multiforme and metastasis in vivo (14). Our own findings in a glioblastoma multiforme in a 10-year-old patient (unpublished data) at a TE of 20 showed the ratio of $I_{1.3}/I_{3.2}$ up to 4.5, and $I_{0.9}/I_{3.2}$ was 1.6. A prominent neutral lipid pattern was present in the proton spectrum at the same TE used in the pilocytic tumors. This significant lipid pattern was not observed in the short-TE spectrum of pilocytic tumors. These results suggest that it may be useful to use short- and long-TE proton MR spectroscopy to characterize astrocytomas in children. Using a TE of 135, Gotsis et al (15) reported that no lipids were detected in benign tumors, such as meningiomas, acoustic schwannomas, pituitary adenomas, pilocytic and low-grade astrocytomas, and oligodendrogliomas. Until now, most lipid measurements in tumors have been done at TEs of 135 to invert the lactate signals (13), which co-resonate at 1.3 ppm with the lipid methylene peak, in order to distinguish between the two. However, MR spectroscopy can maximally detect visible lipid signals with a short TE, and the intensities of lipids can be quantitated relative to Cho with a lesser degree of T2 weighting. In our study, the lipid pattern found in pilocytic astrocytomas was different from that reported in glioblastoma, suggesting that this observation may be used to differentiate benign astrocytomas from malignant tumors. The combination of data from long- and short-TE spectra may be useful for evaluating metabolites and lipids/macromolecules in tumors.

Implications of High Lactate Concentrations in Pediatric Pilocytic Tumors

A wealth of information about brain metabolism may be obtained from proton MR spectroscopy. Findings commonly revealed by this technique include NAA as a putative neuronal marker; Cr/phosphocreatine as an essential energy reservoir; lactate as the end product and a marker for glycolysis; and Cho products as main components of membranes, which may indicate the degree of membrane turnover (16). Among these metabolites, Cho and lactate have received most of the attention in studies of tumors with proton MR spectroscopy. Elevated Cho concentration is often found in tumors, since high Cho implies a rapid turnover of proliferating tumor cells. Lactate is also presumed to provide important information on tumor metabolism, since it is an end product of the anaerobic glycolytic cycle; however, the presence of lactate within a tumor is often overinterpreted as solely the result of tumor necrosis. Correlations between lactate concentration and malignancy are controversial in proton MR spectroscopic studies of tumors. Since Warburg (17) reported that malignant cells have diminished respiratory rates, subsequent studies have pointed out that this is neither a unique pattern nor an essential characteristic of all varieties of cancer (18, 19). It does seem to be true that in most cases in which tumors exhibit a high degree of anaplasia there are rather low levels of respiration and elevated glucose utilization. This is often the result of rapid growth with increased glucose uptake and a decreased number of mitochondria per cell. Using proton MR spectroscopy, Fulham et al (20) reported that lactate occurred in significantly greater amounts in higher grade tumors. However, Negendank et al (21) and Ott et al (22) reported no correlation between lactate and histopathologic grade of tumors. Studies with positron emission tomography (PET) and proton MR spectroscopy have shown elevated lactate in both hyper- and hypometabolic human gliomas. On PET studies with 18F-fluorodeoxyglucose (FDG), high FDG uptake is presumed to be an indicator of increased glycolytic activity (23, 24), which is often observed in malignant tumors (25). Increased glycolysis often accompanies a high concentration of lactate (26). Alger et al (27) and Herholz et al (28) reported finding high lactate concentration in tumors with both high and low FDG uptake using the combined methods of proton MR spectroscopy and PET. Ott et al (22) found both elevated and negligible lactate concentrations among benign tumors by proton MR spectroscopy. Thus, high lactate concentration can be found in both malignant and benign tumors.

An interesting finding in our study was the presence of lactate in measurable concentrations in the pediatric pilocytic astrocytoma. Elevation of lactate in this histologically benign tumor implies reasons other than tumor necrosis. None of our histologic specimens exhibited areas of necrosis. Any concern that lactate in these tumors arose from a response to chemotherapy can be ruled out, since all the studies were performed on patients who had not received chemotherapy at the time of the study. Contamination by metabolites from tumor cysts is less likely because the voxel was placed carefully within the solid portion of the tumor in all nine patients and lactate was found consistently in all patients. On the other hand, lactate elevation of this tumor agrees with results from PET studies in similar tumors (29). Significantly high glucose utilization rates have been found in other benign tumors, indicating that benign tumors may be metabolically active and have high glucose utilization rates, which may be necessary, especially if the metabolic pathways within the pilocytic tumor rely predominantly on anaerobic glycolysis for energy. High glucose utilization is also found in malignant tumors, and corresponds to high glycolytic activities. Another reason for increased glycolytic metabolism may be due to decreased mitochondrial electron transport activities in the tumor, which would decrease the capacity of the oxidative tricarboxylic acid cycle, as suggested by Lichter et al (30). They found increased glucose utilization in pituitary adenomas and schwannomas using FDG-PET. Oxygen consumption studies from isolated mitochondria from these tumors showed no respiration with substrates entering the electron transfer pathway, even though moderately high levels of respiration were seen with ascorbate and N,N,N′,N′-tetramethyl-p-phenylene diamine (TMPD). This suggests that some benign tumors may have decreased electron transport activities, consequently increasing glucose utilization through glycolytic pathways that produce lactate. The unique presentation of the metabolism of the pilocytic astrocytoma eludes a proper explanation for its high glucose utilization and high lactate accumulation seen on PET and proton MR spectroscopic studies.

Conclusion

Our findings suggest that benign pilocytic astrocytomas have high lactate concentrations from as yet unknown biochemical mechanisms. The presence of lactate within pilocytic tumors could be explained by several mechanisms, such as the abnormal number or dysfunction of mitochondria, which would interfere with the process of oxidative phosphorylation and electron transport, alterations in proportional oxygen delivery, and oxygen extraction or usage by tumor or anaerobic glycolysis by tumor cells.

Acknowledgments

We thank the technologists in the MRI Unit at Children's Hospital Medical Center for scanning some of the patients and Douglas L. Rothman at Yale University for reading the manuscript.

References

1. Felix R, Schorner W, Laniado M, et al. **Brain tumors: MR imaging with gadolinium-DTPA.** *Radiology* 1985;156:681–688
2. Behar KL, Rothman DL, Petroff OAC. **Analysis of macromolecule**

resonances in 1H NMR spectra of human brain. *Magn Reson Med* 1994;32:294–302
3. Hwang J-H, Graham GD, Behar KL, Alger JR, Prichard JW, Rothman DL. **Short echo time proton magnetic resonance spectroscopic imaging of macromolecule and metabolite signal intensities in the human.** *Magn Reson Med* 1996;35:633–639
4. Posse S, Schuknecht B, Simth ME, van Zijl PCM, Herschkovitz N, Moonen CTW. **Short echo time proton MR spectroscopic imaging.** *J Comput Assist Tomogr* 1994;17:1–14
5. Howe FA, McLean MA, Sanders DE, et al. **Metabolite nulling in short echo time in vivo 'H MRS of human brain tumors.** Proceedings of the 2nd Annual meeting of the Society of Magnetic Resonance. April, 1995;1705
6. Kuesel AC, Brieere KM, Halliday WC, Sutherland GR, Donnely SM, Smith ICP. **Mobile lipid accumulation in necrotic tissue of high grade astrocytomas.** *Anticancer Res* 1996;16:1485–1490
7. Haase A, Frahm J, Hanike W, Matthaei D. **1H NMR chemical shift selective (CHESS) imaging.** *Phys Med Biol* 1985;30:341–344
8. Bottomly PA. **Selective volume method for performing localized NMR spectroscopy.** US Patent 4 480 228; 1984
9. Kimmich R, Hoepfel D. **Volume selective multipulse spin echo spectroscopy.** *J Magn Reson* 1987;72:379–384
10. Frahm J, Bruhn H, Gyngell MA, Merboldt KD, Hanike W, Sauter R. **Localized high-resolution NMR spectroscopy using stimulated echoes: initial applications to human brain in vivo.** *Magn Reson Med* 1989;9:79–93
11. Sutton LN, Wang Z, Gusnard D, et al. **Proton magnetic resonance spectroscopy of pediatric brain tumors.** *Neurosurgery* 1992;31:195–202
12. Sutton LN, Wehrli SL, Gennarelli L, et al. **High-resolution 1H-magnetic resonance spectroscopy of pediatric posterior fossa tumors in vitro.** *J Neurosurg* 1994;81:443–448
13. Lazareff JA, Olmstead C, Bockhurst K, Alger JR. **Proton magnetic resonance spectroscopic imaging of pediatric low-grade astrocytomas.** *Childs Nerv Syst* 1996;12:130–135
14. Martinez-Perez I, Moreno A, Barba I, et al. **Large lipid droplets observed by electron microscopy in six brain tumors with 'H MRS in vivo pattern.** Proceedings of the 4th Annual Meeting of the International Society of Magnetic Resonance. April, 1996;979
15. Gotsis ED, Fountas K, Kapsalalaki E, Toulas P, Peristeris G, Papadakis N. **In vivo proton MR spectroscopy: the diagnostic possibilities of lipid resonances in brain tumors.** *Anticancer Res* 1996; 16:1565–1568
16. Tedeshi G, Schiffmann R, Barto NW, et al. **Proton magnetic resonance spectroscopic imaging in childhood ataxia with diffuse central nervous system hypomyelination.** *Neurology* 1995;45:1526–1532
17. Warburg O. **On the origin of cancer cells.** *Science* 1956;123:309–314
18. Lichter T, Dohrmann G. **Respiratory patterns in human brain tumors.** *Neurosurgery* 1986;19:898–899
19. Potter VR. **Biochemical perspectives in cancer research.** *Cancer Res* 1964;24:1086–1098
20. Fulham MJ, Bizzi A, Dietz MJ, et al. **Mapping of brain tumor metabolites with proton spectroscopic imaging: clinical relevance.** *Radiology* 1992;185:675–686
21. Negendank W, Sauter R. **Intratumoral lipids in 1H MRS in vivo in brain tumors: experience of the Siemens cooperative clinical trial.** *Anticancer Res* 1996;16:1533–1538
22. Ott D, Hennig J, Ernst T. **Human brain tumors: assessment with in vivo proton MR spectroscopy,** *Radiology* 1993;186:745–752
23. Di Chiro G, deLaPaz RL, Brooks RA, et al. **Glucose utilization of cerebral gliomas measured by [18F] fluorodeoxyglucose and positron emission tomography.** *Neurology* 1982;32:123–129
24. Herholz K, Wienhard, Hiess WD. **Validity of PET studies in brain tumors.** *Cereb Brain Metab Rev* 1990;2:240–265
25. Mahaley MS. **The respiration of normal brain and brain tumors.** *Cancer Res* 1966;26:196–197
26. Staub F, Baethmann A, Peters J, et al. **Effects of lactacidosis on glial cell volume and viability.** *J Cereb Blood Flow Metab* 1990;10: 866–876
27. Alger JR, Frank JA, Bizzi A, et al. **Metabolism of human gliomas: assessment with H-1 MR spectroscopy and F-18 fluorodeoxyglucose PET.** *Radiology* 1990;177:633–641
28. Herholz K, Heindel W, Layton PR, et al. **In vivo imaging of glucose consumption and lactate concentration in human gliomas.** *Ann Neurology* 1992;31:319–327
29. Fulham MJ, Melisi JW, Nishimiya J, Dwyer AJ, Di Chiro G. **Neuroimaging of juvenile pilocytic astrocytomas: an enigma.** *Radiology* 1993;189:221–225
30. Lichter T, Dohrmann GJ, Gets GS. **Respiratory deficiency and increased glycolysis in benign human tumors.** *Surg Forum* 1984;35: 486–488